

# Evolutionary Patterns of Shape and Functional Diversification in the Skull and Jaw Musculature of Triggerfishes (Teleostei: Balistidae)

Charlene L. McCord<sup>1,2\*</sup> and Mark W. Westneat<sup>1,2</sup>

<sup>1</sup>*Department of Organismal Biology and Anatomy, University of Chicago, Chicago, Illinois 60637*

<sup>2</sup>*Field Museum of Natural History, Division of Fishes, Chicago, Illinois 60605*

**ABSTRACT** The robust skull and highly subdivided adductor mandibulae muscles of triggerfishes provide an excellent system within which to analyze the evolutionary processes underlying phenotypic diversification. We surveyed the anatomical diversity of balistid jaws using Procrustes-based geometric morphometric analyses and a phylomorphospace approach to quantifying morphological transformation through evolution. We hypothesized that metrics of interspecific cranial shape would reveal patterns of phylogenetic diversification that are congruent with functional and ecological transformation. Morphological landmarks outlining skull and adductor mandibulae muscle shape were collected from 27 triggerfish species. Procrustes-transformed skull shape configurations revealed significant phylogenetic and size-influenced structure. Phylomorphospace plots of cranial shape diversity reveal groupings of shape between different species of triggerfish that are mostly consistent with phylogenetic relatedness. Repeated instances of convergence upon similar cranial shape by genetically disparate taxa are likely due to the functional demands of shared specialized dietary habits. This study shows that the diversification of triggerfish skulls occurs via modifications of cranial silhouette and the positioning of subdivided jaw adductor muscles. Using the morphometric data collected here as input to a biomechanical model of triggerfish jaw function, we find that subdivided jaw adductors, in conjunction with a unique cranial skeleton, have direct biomechanical consequences that are not always congruent with phylomorphospace patterns in the triggerfish lineage. The integration of geometric morphometrics with biomechanical modeling in a phylogenetic context provides novel insight into the evolutionary patterns and ecological role of muscle subdivisions in triggerfishes. *J. Morphol.* 277:737–752, 2016. © 2016 Wiley Periodicals, Inc.

**KEY WORDS:** phylomorphospace; jaw biomechanics; functional morphology; adductor mandibulae

## INTRODUCTION

Understanding phenotypic diversification is a central objective in the field of evolutionary biology. The resurgence of quantitative morphological analyses in recent years highlights one way of using the phenome, or a collection of an organism's phenotypic characters, as a way to understand the

evolution of the genome (Burleigh et al., 2013). This “phenomic revolution” has catalyzed the development of a wide range of new techniques for imaging, quantifying and comparing anatomical detail in a biologically relevant way. Used in conjunction with molecular phylogenetics, the ever-broadening suite of powerful modern methods for analyzing organismal morphology has played an integral role in quantitative comparative analyses of ontogeny, biomechanical function, scaling, and evolution of complex phenotypes. The architecturally complex skulls of fishes have often yielded insight into the evolution of shape within a phylogenetic context (i.e., Winterbottom, 1974; Schaefer and Lauder, 1996; Collar et al., 2005; Sidlauskas, 2008; Cooper and Westneat, 2009). This study focuses on the globally distributed family Balistidae, which are an excellent system in which to explore the morphometric evolution of the skull.

The Balistidae are a morphologically conspicuous group of temperate and tropical marine fishes (Kuitert and Debelius, 2007), with well-resolved phylogenetic relationships (Santini et al., 2013; McCord and Westneat, 2016). The 42 triggerfish species in this family are typically solitary diurnal predators, and exhibit an exceptional range of ecological diversity (Carpenter and Niem, 1999). One

Additional Supporting Information may be found in the online version of this article.

Contract grant sponsor: NSF Integrative Graduate Education and Research Traineeship Grant; Grant numbers: DGE-0903637, DEB 1447321, DEB 0844745; Contract grant sponsors: a 2011 NSF EAPSI Grant; the 2013 Field Museum Women's Board Fellowship.

\*Correspondence to: Charlene L. McCord, Department of Organismal Biology and Anatomy, University of Chicago, Chicago, Illinois 60637. E-mail: Charlene.L.McCord@gmail.com

Received 27 October 2015; Revised 17 February 2016; Accepted 21 February 2016.

Published online 20 March 2016 in Wiley Online Library (wileyonlinelibrary.com). DOI 10.1002/jmor.20531

of the most distinctive features of balistid fishes are their small, powerful oral jaws that are used to capture and process a variety of prey items ranging from algae to hard-shelled mollusks (Turingan and Wainwright, 1993; Wainwright and Turingan, 1993; Turingan, 1994). Indeed, the anatomy, function, ontogeny, and evolution of the bones and muscles that are associated with the triggerfish feeding apparatus have been extensively studied (i.e., Winterbottom, 1974; Turingan, 1994; Friel and Wainwright, 1997, 1999; Wainwright and Friel, 2000;), although a detailed morphometric approach has not yet been applied to this group. Unlike the highly kinetic skulls of most teleost fishes, triggerfishes have a maxilla that is fused to the premaxilla on each side of the head, and possess a small number of robust teeth, two features that are thought to magnify bite force for duraphagous feeding by providing a sturdy frame upon which large jaw adductor muscles can pull. As in other fishes, the adductor mandibulae muscles insert onto the lower jaw and are responsible for generating bite force in triggerfishes (Gregory, 1933; Lauder, 1985). However, in stark contrast to the typical teleost adductor mandibulae muscle complex that consists of three major muscle subdivisions, the jaw closing muscles of triggerfishes have been physically subdivided through evolution resulting in a total of six adductor mandibulae muscles; four that insert onto the lower jaw while the remaining two subdivisions attach to the upper jaw. While the gross anatomy of these highly subdivided jaw adductor muscles is well documented, the details of interspecific muscle subdivision and skull shape variability, and the biomechanical consequences thereof, have yet to be investigated. Multiple muscle subdivisions in this system raise intriguing questions about the causes and effects of the process of subdivision in vertebrate cranial muscles.

The nature of morphological diversity is best addressed within a morphospace (Foote, 1997; Stayton, 2005). Recent advances in the methods and tools available for geometric morphometric analyses permit quantifying and comparing shape change in two or three dimensions (e.g., Ming and Xing-Re, 2014; Olsen and Westneat, 2015) and for investigating shape transformations within the context of phylogeny (e.g., Tsuboi et al., 2014), ecology (e.g., Bjarnason et al., 2015), size (e.g., Openshaw and Keogh, 2014), ontogeny (e.g., D'Amore, 2015), or other factors that influence shape diversification in vertebrates. In this project, we developed a novel 2D landmark-based morphometrics protocol that not only outlines the skeletal silhouette of the triggerfish cranium, but also frames the moving parts of the skull and the gross architecture of the six adductor mandibulae subdivisions. The triggerfishes are an ideal group for two-dimensional morphometrics due to their

flat profile (e.g., there is a negligible medial-lateral component to the trajectory of adductor mandibulae musculature from origin to insertion). By quantifying both the static and moveable elements of the triggerfish cranial configuration, the coordinate data depicts the geometry of basic shape features and functionally relevant components of the skull. Utilizing the geometric configurations of muscles, bones, and joints, we employed biomechanical modeling to estimate simple measures of the biomechanical capabilities of the unique triggerfish jaw system. We hypothesized that major axes of cranial morphometric diversity, analyzed in a phylomorphospace, correspond with major phylogenetic groups and with features of feeding biomechanics in this group. Alternatively, we anticipated that triggerfishes might show convergence across phylogenetic groups.

Biomechanical models promote an understanding of the anatomical basis of feeding behavior and provide a way of investigating the functional consequences of interspecific morphological variation (Westneat, 2004). Here, we focus on the mechanical advantage of the upper and lower jaws, which is calculated as the ratio of in-lever to out-lever (Barel, 1982; Biewener, 1989; Westneat, 1994). Because of their hard biting feeding behavior, we predicted that triggerfish jaw levers will have high mechanical advantage for both the upper and lower jaws.

This project combines Procrustes-based geometric morphometrics, biomechanical modeling, and phylogenetic comparative methods to gain an understanding of morphological diversification of triggerfish cranial shape that is functionally relevant. The objectives of this study were to: 1) dissect, photograph, and describe the cranial morphology of triggerfishes using the nomenclature of Datovo and Vari (2013); 2) use geometric morphometrics to explore the influence of size and phylogeny on triggerfish cranial shape variability; 3) use biomechanical modeling to evaluate the functional consequences of the unique trophic anatomy of triggerfishes and trace phylogenetic changes in jaw biomechanics; and 4) visualize the evolutionary patterns of cranial shape diversification among close relatives and test for patterns of convergence across clades of triggerfishes using a phylomorphospace approach.

## METHODS

### Geometric Morphometrics

Several hypotheses on adductor mandibulae homology have been put forth based on the relative origins and insertions of muscle subdivisions (Winterbottom, 1974), origins and relative muscle mass (Friel and Wainwright, 1997), the path of the *ramus mandibularis trigeminus* (Nakae and Sasaki, 2004), and muscular ontogeny (Konstantinidis and Harris, 2011). Most recently, Datovo and Vari (2013) proposed a simplified, novel approach to the identification and naming of

TABLE 1. Summary of the various hypotheses of triggerfish adductor mandibulae muscle homologies

Datovo and Vari	Konstantinidis and Harris	Nakae and Sasaki	Friel and Wainwright	Winterbottom
2013	2011	2008	1997	1974
Relative position	Development of AM	AM innervation	Origins, insertions & relative mass	Insertions & origins
Epirictalis <sup>a</sup>	AM $\alpha'$	A2 $\beta$	A2 $\beta'$ b	A2 $\beta$
Subrictalis <sup>a</sup>	AM $\alpha''$	A2 $\gamma$	A2 $\beta''$ b	A2 $\gamma$
Substegalis	AM $\alpha'''$	A3 $\alpha$	A3	A3
Retromalaris	AM $\beta'$	A2 $\alpha$	A2 $\alpha$	A2 $\alpha$
Promalaris	AM $\beta''$	A1	A1 $\alpha$ b	A1 $\alpha$
Epistegalis	N/A	A3 $\beta$	A1 $\beta$ b	A1 $\beta$

<sup>a</sup>Our proposed naming scheme for two muscle subdivisions in triggerfishes that both originate along the horizontal portion of the preopercle bone and are positioned on top of one another. The epirictalis is present in all tetraodontiform fishes, whereas the subrictalis is unique, as far as we know, to the triggerfishes and select filefishes.

homologous adductor mandibulae muscles that: 1) is applicable to all teleosts; 2) uses intuitive positional-based terminology to name jaw adductor muscle subdivisions; and 3) is easily adaptable for instances of evolutionary subdivision and/or coalescence of muscle subdivisions. Here, we utilize Datovo and Vari's myological nomenclature to explore triggerfish cranial shape diversification and propose a new naming convention for two unique subdivisions within the triggerfish lineage (Table 1).

Seventy-nine formalin-fixed, alcohol-preserved adult triggerfish specimens were selected, mostly from the Fishes Collection at the Field Museum of Natural History. Additional specimens were provided by the United States National Museum of Natural History, the Taiwan National Museum of Marine Biology and Aquarium, and the Taiwan Biodiversity Research Center of the Academia Sinica. At least two, and often several, adult specimens from each of the triggerfish genera were examined (Table 2) except in the case of the rare genus, *Xenobalistes*, for which a specimen was not available for dissection. The triggerfish taxonomic names utilized here follow those outlined in McCord and Westneat (2016).

Dissections were performed on the right side of each specimen's head in order to expose morphological landmarks that encapsulate cranial geometry and outline functionally relevant elements of the skull (Fig. 1a). Anatomy was identified using the adductor mandibulae naming conventions of Datovo and Vari (2013), the hyoid muscle nomenclature of Winterbottom (1974), and the osteological and connective tissue terminology of Tyler (1980). Cranial dissections were documented in two photographs per fish (one to capture superficial cranial landmarks, and a second to detail deep landmarks) in lateral view at a fixed zoom and distance using a Nikon D3100 digital camera. To maintain identical positioning of all cranial elements for photograph superimposition and subsequent geometric morphometric analyses, all fishes were photographed with their mouths closed from a position directly perpendicular to the plane of the morphological landmarks on the side of each specimen's head. A scale bar was included in each photograph. Superficial and deep dissection photographs were aligned using the "Auto-Align Layers" function in Adobe Photoshop CS5 and single, layered photographs for each dissected fish were created. The (x, y) coordinates of forty-four (44) type I (a landmark whose claimed homology between cases is supported by the strongest evidence) and type II (a landmark whose claimed homology is supported only by relative geometric evidence) homologous morphological landmarks were digitized on each photograph using the software program tpsDig (Bookstein, 1997; Rohlf, 2010; see Fig. 1). The entire set of Cartesian coordinates for all landmarks outline the cranium and associated functionally relevant elements of the skull that, together, form the geometric morphometric data for this study. Morphometric landmark data and scaling factors were submitted in tabular form to the Dryad Digital Repository: <http://dx.doi.org/10.5061/dryad.vd7bf>.

To reduce differences in landmark configurations that are due to variation in the size of the specimens used, or their relative position when photographed, geometric morphometric coordinate data for all specimens was projected into tangent shape-space using full Procrustes superimposition (Klingenberg, 2008). Generalized procrustes analysis (GPA) methods scale, rotate, and translate landmarks such that the squared, summed distances between corresponding landmarks of each individual and the mean skull shape are minimized without distorting shape information, and calculates the centroid size of each specimen, which is a measure of relative size (Bookstein, 1997; Zelditch et al., 2004). Procrustes-transformed shape coordinates and centroid size were calculated for all 79 specimens in the dataset and used for all subsequent analyses.

## Phylogenetic Relationships of the Triggerfishes

This study used a recent reconstruction of the phylogenetic relationships of balistoid fishes as a framework for the phylogenetic analyses of cranial shape and jaw biomechanics presented here (McCord and Westneat, 2016). A topology of relationships for triggerfishes was extracted from this larger study based on three nuclear markers (*bmp4*, *rag2*, and *tmo4c4*) and two mitochondrial regions (*12S* and *16S*) plus all available sequences for *cytB*, *rag1*, *COI* and rhodopsin from GenBank, with the matrix containing 27 triggerfish species. A 10 million generation MrBayes 3.2.2 XSEDE run on the CIPRES Science Gateway was conducted using the concatenated DNA supermatrix as input. All shape analyses discussed below are based on the topology and branch length data from the maximum posterior-probability triggerfish tree that was calculated from all post burn-in trees (Fig. 2). The phylogeny used in this study is available on the Dryad Digital Repository: <http://dx.doi.org/10.5061/dryad.vd7bf>.

## Effects of Size and Phylogeny on Triggerfish Cranial Shape

The potential influence of size variation in GPA-transformed shape data was tested by performing a series of multivariate regressions of shape on log-transformed centroid size (Monteiro, 1999). All geometric morphometric, phylomorphospace analyses, and statistical tests were conducted using the comprehensive software package MorphoJ (Klingenberg, 2011; [http://www.flywings.org.uk/MorphoJ\\_page.htm](http://www.flywings.org.uk/MorphoJ_page.htm)). A permutation test with 10,000 replications was included to assess the statistical significance of two such multivariate regressions; the first without considering phylogenetic structure, and a second that was pooled within each species so as to account for any potential phylogenetic component to the relationship of GPA shape and centroid size. As is common in geometric morphometric analyses where size is shown to have a significant influence on patterns of shape variation, the residuals of the unpoled

TABLE 2. Taxa used in this project, species ID, and the range of specimen standard lengths in centimeters

Species ID	Species name	No. of specimens	SL (cm)	Upper jaw MA	Lower jaw MA	Specimen catalog #
1	<i>Abalistes stellatus</i>	2	13.7–20.5	0.77 ± 0.17	0.45 ± 0.04	NMNH 349664
2	<i>Balistapus undulatus</i>	3	9.1–12.4	0.62 ± 0.02	0.56 ± 0.08	FMNH 124004, 124009, 123991
3	<i>Balistes capricus</i>	3	18.6–21.6	0.55 ± 0.04	0.47 ± 0.02	AQU 1, FMNH 64243, 46692
4	<i>Balistes polylepis</i>	3	15.9–17.5	0.71 ± 0.02	0.49 ± 0.03	FMNH 73535; NMNH 397353, 397352
5	<i>Balistes punctatus</i>	2	15.4–16.8	0.72 ± 0.01	0.44 ± 0.02	NMNH 193915
6	<i>Balistes vetula</i>	3	9.5–11.6	0.69 ± 0.05	0.52 ± 0.04	FMNH 47961; NMNH 397341
7	<i>Balistoides conspicillum</i>	3	12.4–14.6	0.63 ± 0.08	0.45 ± 0.02	FMNH 126094, 120557; NMNH 191199
8	<i>Pseudobalistes viridescens</i>	2	11.6–21.4	0.69 ± 0.01	0.45 ± 0.02	FMNH 121698, 121699; NMNH 142960
9	<i>Canthidermis maculata</i>	3	8.4–13.7	0.71 ± 0.04	0.45 ± 0.03	FMNH 119547, 4882; NMNH 142951
10	<i>Canthidermis sufflamen</i>	2	9.2–17.9	0.58 ± 0.01	0.41 ± 0.02	FMNH 72523, 46693
11	<i>Melichthys niger</i>	3	15.6–17.2	0.67 ± 0.09	0.48 ± 0.06	AQU 2; FMNH 119588, 118789
12	<i>Melichthys viatua</i>	3	13.1–14.6	1.07 ± 0.22	0.48 ± 0.12	FMNH 124014, 120079, 121208
13	<i>Odonus niger</i>	3	12.2–14.9	0.67 ± 0.04	0.65 ± 0.06	FMNH 118793, 118794; NMNH 372754
14	<i>Pseudobalistes flavimarginatus</i>	3	10.9–12.9	0.82 ± 0.09	0.48 ± 0.02	AQU 3; FMNH 120558; NMNH 142966
15	<i>Balistes fuscus</i>	4	9.5–14.6	0.86 ± 0.05	0.48 ± 0.02	AQU 4; NMNH 349719
16	<i>Balistes naufragium</i>	3	12.3–15.2	0.71 ± 0.08	0.46 ± 0.01	FMNH 32010, NMNH 367905
17	<i>Rhinecanthus aculeatus</i>	3	14.2–15	0.75 ± 0.02	0.45 ± 0.03	FMNH 16396, 16397, 63521
18	<i>Rhinecanthus assasi</i>	3	16.3–17.3	0.77 ± 0.08	0.51 ± 0.03	AQU 5; NMNH 166902
19	<i>Rhinecanthus rectangulus</i>	4	14.9–16.3	0.74 ± 0.05	0.42 ± 0.01	FMNH 44229, 118797, 47727
20	<i>Rhinecanthus verrucosus</i>	2	11.1–13.2	1.02 ± 0.01	0.47 ± 0.04	FMNH 120082; NMNH 114873
21	<i>Sufflamen bursa</i>	5	9.6–12.6	0.72 ± 0.02	0.33 ± 0.03	FMNH 124026, 119551; NMNH 6454
22	<i>Sufflamen chrysopterum</i>	3	12.5–15.9	0.71 ± 0.08	0.48 ± 0.07	FMNH 119551, 120075; NMNH 113089
23	<i>Sufflamen fraenatum</i>	3	13.2–16	0.84 ± 0.12	0.40 ± 0.03	NMNH 305948, 396821
24	<i>Sufflamen verres</i>	3	11.6–13.6	0.68 ± 0.07	0.36 ± 0.03	FMNH 41747, 41748; NMNH 65432
25	<i>Xanthichthys auromarginatus</i>	3	11.6–13.9	1.07 ± 0.03	0.35 ± 0.04	FMNH 118800; NMNH 305263
26	<i>Xanthichthys mento</i>	3	13.1–17	0.81 ± 0.09	0.49 ± 0.09	FMNH 1781; NMNH 126166
27	<i>Xanthichthys ringens</i>	2	11–13.7	0.67 ± 0.01	0.62 ± 0.01	NMNH 360707, 360707

regression of shape on size were used for further description and visualization of interspecific triggerfish cranial shape divergence. This data will hereafter be referred to as, “size-corrected cranial shape” (Klingenberg and Monteiro, 2005; Drake and Klingenberg, 2010; Openshaw and Keogh, 2014).

To test for the presence of phylogenetic signal in GPA size-corrected shape data, the multivariate Tree length permutation test of Klingenberg and Gidaszewski (2010) with 10,000 replications was used. This test uses maximum parsimony to map shape scores onto the tips of a phylogeny by finding the set of internal node shape values that minimize the sum of squared Procrustes distances over all branches of the phylogeny. The Tree length test compares the actual distribution of terminal node shape scores to those obtained by randomly assigning shape values to terminal nodes, which is a simulation of no phylogenetic signal. The permutation test returns a *P* value that represents the proportion of randomly permuted shape datasets that have a sum of squared Procrustes distance changes that is shorter than or equal to the value for the original shape data (Klingenberg and Gidaszewski, 2010).

### Description and Visualization of Interspecific Cranial Shape Variation

After generalized procrustes analysis, size-corrected procrustes coordinates were averaged by species and a principal components analysis (PCA) was performed to determine the axes of maximal shape variation. By plotting the principal component score for all taxa, the location of each species’ mean size-corrected cranial shape in two-dimensional morphospace was identified and used to establish general patterns of inter-

specific cranial shape differences (Bookstein, 1997; Zelditch et al., 2004). To compare the relative amount of size-corrected cranial shape variation in the two major triggerfish clades, the coefficient of variation for the pooled set of size-corrected PC scores was calculated for all taxa in each clade separately. We chose to examine the first three PC axes that, together, accounted for the greatest proportion of overall size-corrected shape variation in the size-corrected data. Wireframe diagrams were used to visualize the patterns of shape change along relevant PC axes.

The statistical significance of interspecific shape variation was quantified using canonical variate and discriminant function analyses. The Procrustes and Mahalanobis distances between size-corrected species’ mean cranial shape were calculated using canonical variate analysis, and a permutation test with 10,000 iterations for all pairwise Procrustes and Mahalanobis distances determined the statistical significance of the differences of size-corrected shape values. Discriminant function analysis was used to determine the reliability of all pairwise between-species shape separation using leave-one-out cross-validation classification as a third measure of between-species shape differentiation (Klingenberg et al., 2012).

Traditional geometric morphometric analyses were combined with phylogenetic comparative methods in order to identify and account for the effects of shared evolutionary history in our study of morphological diversification, and to reconstruct the

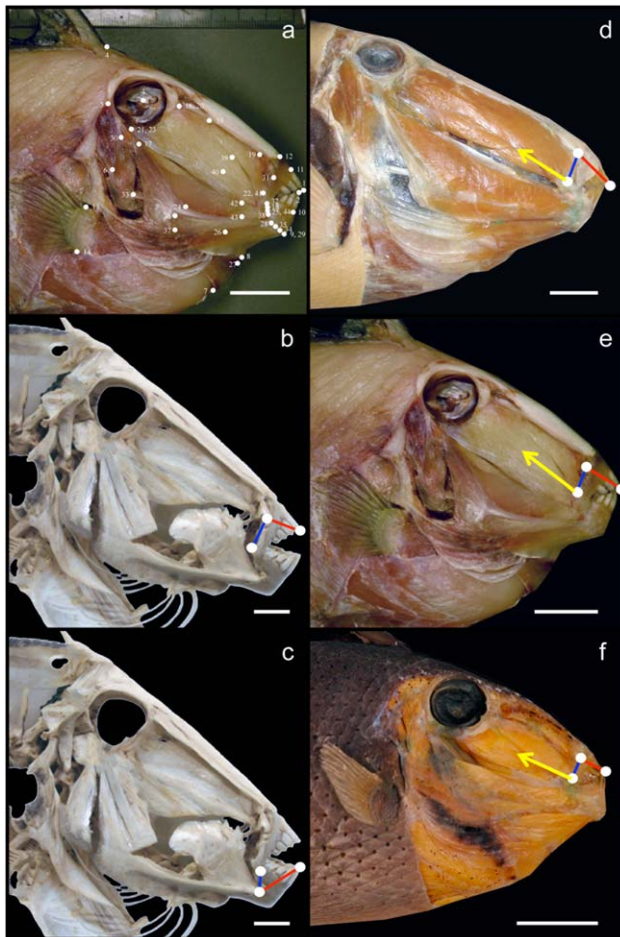


Fig. 1. a) Anatomical landmarks used for geometric morphometric analyses diagrammed on a fresh *Balistes capriscus* specimen. Protractor hyoidei superficialis was removed to show deep hyoid musculature. Landmarks are as follows: 1. tip of upper teeth; 2. tip of lower teeth; 3. center of eye; 4. rostral-most point of trigger; 5. dorsal, medial levator operculi; 6. ventral, medial levator operculi; 7. junction of hyohyoideus and sternohyoideus; 8. junction of hyohyoideus and protractor hyoidei; 9. junction of dentary and protractor hyoidei; 10. midline junction of dentary and teeth; 11. junction of premaxilla and teeth; 12. junction of maxilla and ethmoid; 13. dorsal tip of pectoral fin; 14. ventral tip of pectoral fin; 15. anterior-most retromalaris origin; 16. mid-retromalaris origin; 17. posterior-most retromalaris origin; 18. retromalaris insertion; 19. anterior-most origin of promalaris; 20. mid-origin of promalaris; 21. anterior-most origin of promalaris; 22. promalaris insertion; 23. epipectalis dorsal origin; 24. epipectalis ventral origin; 25. epipectalis insertion; 26. dorsal origin of protractor hyoidei superficialis; 27. ventral origin of protractor hyoidei superficialis; 28. quadrate-articular jaw joint; 29. ventral insertion of protractor hyoidei superficialis; 30. hyomandibular-opercle joint; 31. palatine-premaxilla jaw joint; 32. maxillomandibular ligament; 33. interoperculomandibular ligament attachment to opercle; 34. connection of mandible and interopercular; 35. dorsal insertion of protractor hyoidei superficialis; 36. dorsal origin of subtrictalis; 37. ventral origin of subtrictalis; 38. insertion of subtrictalis; 39. dorsal epistegalis origin; 40. ventral epistegalis origin; 41. epistegalis insertion; 42. dorsal substegalis origin; 43. ventral substegalis origin; 44. substegalis insertion. **b-f**) Diagrams outlining the functionally relevant landmarks associated with upper-jaw closing in representative triggerfishes with different feeding ecology and jaw biomechanics schematic on skeleton of *Balistes capriscus* highlighting all measurements needed to calculate the MA of the upper and lower jaw on any triggerfish. **b**) upper jaw MA schematic; **c**) lower jaw MA schematic; **d**) *Rhinecanthus aculeatus*, generalist; **e**) *Balistes capriscus*, durophagous; **f**) *Xanthichthys ringens*, algae/plankton. Red lines: outlever; blue lines: in-lever; yellow arrow: promalaris line of action; green arrow: retromalaris line of action. White circles indicate the location of the palatine-premaxilla jaw joint, the tip of the anterior most upper tooth, and the muscle insertion sites. White scale bar = 2 cm. Protractor hyoidei superficialis has been removed in all fishes above. Retromalaris muscle was removed in *Rhinecanthus aculeatus* and *Xanthichthys ringens* to allow an unobstructed view of the entire promalaris subdivision.

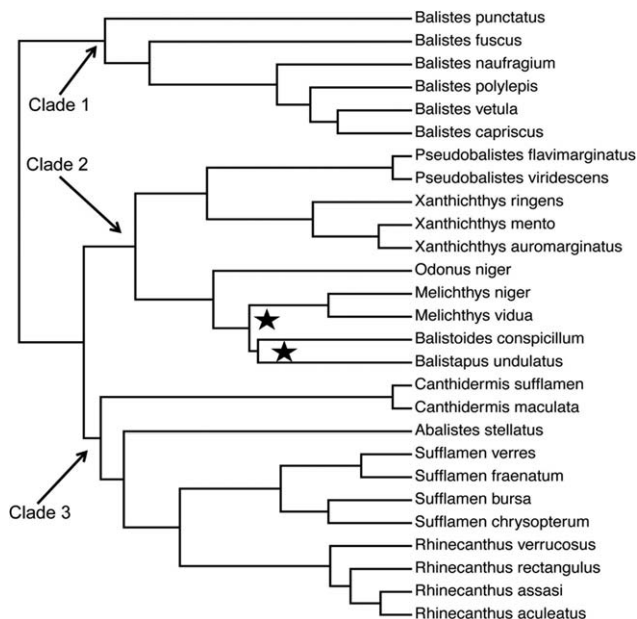


Fig. 2. Ultrametrized triggerfish Bayesian maximum posterior probability phylogeny used for all phylogenetic comparative methods in this study. The two black stars mark the only nodes with PP < 99%.

history of shape changes in the triggerfish lineage. To visualize cranial shape as it relates to phylogeny, we created a phylomorphospace plot by projecting the triggerfish phylogeny into tangent shape space using weighted squared-change parsimony, and plotted the resultant tree for the first three PCs of the size-corrected species mean shape scores (Maddison, 1991; Klingenberg and Ekau, 1996; Sidlauskas, 2008; Klingenberg and Gidaszewski, 2010). These methods also reconstructed size-corrected cranial shape at each internal node. Using these ancestral states, we were able to visualize major changes in the direction and magnitude of shape differentiation along the branches of the triggerfish phylogeny and conduct an evolutionary PCA (EPCA) to identify the shape features that account for the greatest amount of shape change along the branches of the triggerfish tree and visualize them using wireframe diagrams (Klingenberg and Gidaszewski, 2010; Muschick et al., 2012). Whereas a traditional PCA rotates the entire shape data configuration to maximize overall geometric variation, EPCA rotates the collective size-corrected cranial shape data to maximize evolutionary shape changes that are reconstructed along the branches of a phylogeny (Schlick-Steiner et al., 2006).

Potential convergences in cranial shape across clades were identified by examining the phylomorphospace plot for taxa near each other in morphospace but from different parts of the phylogeny. Three candidate species pairs were identified for convergence testing: *Pseudobalistes flavimarginatus* + *Balistes fuscus*, *Canthidermis maculata* + *Melichthys niger*, and *Balistapus undulatus* + *Sufflamen fraenatum*. To statistically test whether convergence in these focal pairs was greater than expected by chance, the phylogeny with branch lengths and scores for PC1 and PC2 were analyzed using the Wheatshaf Index in the R package Windex (Arbuckle et al., 2014), with these three species pairs indicated as focal species.

## Biomechanical Analyses

Scaled coordinate data were used as input for a simple static jaw model that predicts the force-transmission capacity of trig-

gerfish jaws. Based on the relative 2D ( $x, y$ ) coordinates of the palatine-premaxilla and quadrate-articular jaw joints, the location of muscle insertion onto the jawbones for the largest muscle mass connecting to the upper and lower jaws (promalaris insertion site and retromalaris insertion point, respectively), and the tips of the teeth, we calculated the morphological mechanical advantage (MA) for both the upper and lower jaws of all species. The 3<sup>rd</sup> dimension is often important when estimating mechanical parameters of biological systems, and there are excellent tools for 3D-morphometrics and 3D-biomechanical modeling that have recently become available (e.g., MorphoJ and StereoMorph). However, for the triggerfishes, we chose to utilize 2D jaw biomechanics because there are no significant muscular pathways into and out of the plane of focus for our anatomical images or morphometric landmark configurations that, together, supply the lever measurements used to calculate the biomechanical variables discussed here. The highest angle out of the plane in triggerfishes is 10°, which may result in up to a 1.5% error in our calculations of jaw mechanical advantage. Morphological mechanical advantage is the ratio of the in-lever to the out-lever. To identify and interpret phylogenetic patterns of balistid jaw biomechanics evolution, we divided the continuous species average MA values into three discrete states (high MA, medium MA, and low MA) using gap coding (see Archie, 1985 for various methods), and then reconstructed ancestral states using maximum likelihood methods in the phytools package for R under an “all rates different (ARD)” transition probability model (Revell, 2012). Species average lever measurements and mechanical advantage calculations are presented in tabular form in the Dryad Digital Repository: <http://dx.doi.org/10.5061/dryad.vd7bf>.

## RESULTS

### Triggerfish Cranial Morphology

All triggerfishes included in this project had similar gross cranial anatomy (Fig. 3). Exploratory dissections revealed several noteworthy associations between the skull and the muscles by which the skull shape has been molded through evolution. Numerous skull and jawbone fusions were evident (see Gregory, 1933 for an exhaustive analysis of triggerfish cranial osteology), providing a robust series of strong anchors for the large and powerful adductor mandibulae muscle subdivisions that function together to close the jaws. The maxilla and mandible were found to be anatomically connected in all specimens by a flat short maxillomandibular ligament. The maxillomandibular ligament has been observed in several groups of fishes and is known to couple mandibular depression with maxillary swing when present (Lauder, 1979). Also unique to the balistid cranium is the anatomical configuration of and rotational dynamics about the upper (palatine-premaxilla) jaw joint. Unlike the highly mobile upper jaw that is common in teleosts, balistids have stabilizing palatine-premaxilla and maxillomandibular ligaments that constrain translocation of the upper jaw during jaw rotation. The upper jaw joint is further steadied by a laterally projecting eminence on the dorsal end of the maxilla (positioned ventral to the palatine) that limits dorsal shifting of the upper jaw during jaw rotation about the palatine. Considered together, this joint anatomy suggests that

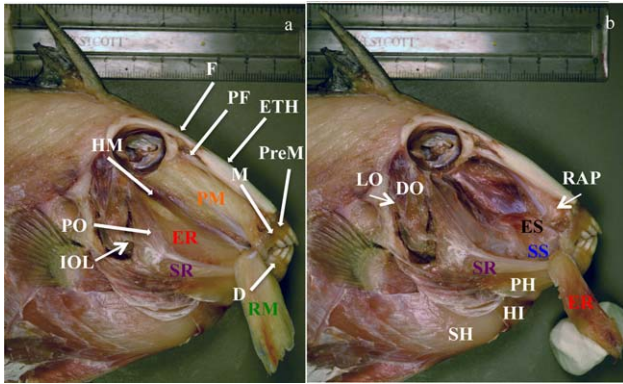


Fig. 3. Triggerfish cranial anatomy as revealed during a detailed dissection of a fresh *Balistes capriscus* specimen. **a)** Superficial adductor mandibulae subdivisions, skull bones and ligamentous attachment between opercular series and lower jaw (white); **b)** Promalaris and retromalaris muscles removed and epirictalis reflected to show deep adductor mandibulae subdivisions and other cranial muscles relevant to the jaw opening and closing mechanism (white); **c)** Photograph of the maxillomandibular ligament, which connects the maxilla and mandible. Adductor mandibulae subdivisions are color-coded as they appear here in all figures that follow. LO = levator operculi; DO = dilatator operculi; IOL = interopercularmandibular ligament; SH = sternohyoideus; HI = hyohyoideus inferioris; PH = protractor hyoidei; RAP = retractor arcus palatini; PM = promalaris (orange); ER = epirictalis (red); SR = subtrictalis (purple); RM = retromalaris (green); ES = epistegalis (black); SS = substegalis (blue); F = frontal; PF = prefrontal; ETH = ethmoid; PreM = premaxilla; M = maxilla, D = dentary; PO = preopercle; HM = hyomandibular.

the upper jaw joint functions as a hinge with negligible dorsoventral movement about the palatine-premaxilla jaw joint during jaw closing.

The adductor mandibulae musculature of triggerfishes was large, highly subdivided, and architecturally complex. Each fish had two muscles that anatomically converge to insert onto the maxilla via a shared tendon: the superficially positioned promalaris (most commonly referred to as the A1 or A1 $\alpha$  subdivision), and the deep epistegalis (A1 $\beta$ ) muscle (Table 1). The promalaris is a large muscle originating along the ventrolateral surface of the ethmoid and prefrontal, as well as dorsal portions of the hyomandibular bone. The epistegalis is small, entirely hidden beneath the promalaris muscle, and originates along the pterygoid bones. The remaining four adductor mandibulae muscles insert along the dorsomedial face of the dentary. The retromalaris (formerly A2 $\alpha$ ) is a large superficial muscle that originates on the ethmoid, prefrontal, and lateral hyomandibular and converges on a tendonous insertion site. The epirictalis is a new muscle name proposed here, to join the Datovo and Vari (2013) naming system, for a unipennate subdivision unique to Tetraodontiformes (formerly A2 $\beta$ ) that originates on the anterior hyomandibular and dorsal preopercle. In addition to inserting onto the dentary, both the retromalaris and epirictalis subdivisions have

fibers that are directly attached to the maxillomandibular ligament, which is the connective tissue that links the upper and lower jaws. The subtrictalis (also proposed here as a name for the muscle unique to triggerfishes that is often termed the A2 $\gamma$ ) is small and originates along the ventrolateral portion of the preopercle and inserts on the back of the mandible. Unlike the other muscles in the triggerfish adductor mandibulae complex, the pennation of the subtrictalis varies interspecifically, occurring in some specimens as a parallel muscle (e.g., *Rhinecanthus aculeatus*), in others as a unipennate muscles (e.g., *Balistapus undulatus*), and a bipennate muscle in still others (e.g., *Balistes polylepis*). Lastly, the substegalis (A3 subdivision) is a small, deep muscle that originates along the quadrate and metapterygoid bones and its fibers converge to insert on the medial face of the mandible.

### Effects of Size and Phylogeny on Triggerfish Cranial Shape

Both size and phylogeny were found to significantly influence the patterns of cranial shape transformation in triggerfishes. After Procrustes superimposition, size accounts for 5.523% ( $P = 0.0004$ ) of overall variation in the geometric morphometric dataset. The regression between size and shape of the pooled-within-species sample suggests the presence of a strong evolutionary allometric signal in cranial shape and accounts for an additional 1.024% ( $P < 0.0001$ ) of total variation. Because size was found to have a significant effect on cranial shape changes within the triggerfish lineage, all analyses that follow utilize the residuals of multivariate regression of Procrustes-transformed shape on log centroid size. The *Tree length* permutation test suggests there is also significant phylogenetic structure in triggerfish cranial shape data ( $P < 0.0001$ ), highlighting the importance of considering the shared evolutionary history of the triggerfishes in the interpretation of the patterns of cranial shape differentiation in size-corrected shape data.

### Divergence and Convergence of Cranial Shape Variation

Phylomorphospace plots show that the triggerfish lineage has spread into a limited, T-shaped region of cranial morphospace (Fig. 4). Each species' relative position in the first three axes of phylomorphospace is generally a good indicator of the statistical significance of interspecific size-corrected shape distances, and all multivariate diversity measures (i.e., canonical variate analysis and leave-one-out cross-validation discriminant function analysis) present equivalent results (Supporting Information). We found a disparity (e.g., inequality) in the amount of shape variation among the three triggerfish clades, with Clade 2

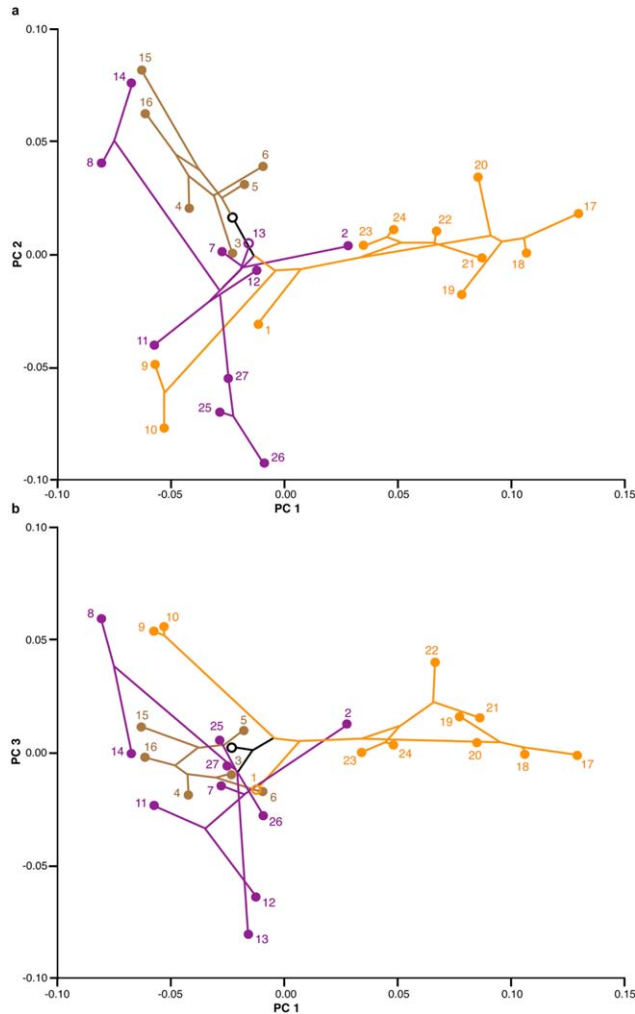


Fig. 4. Phylomorphospace plot of **a)** PC1 vs PC2; and **b)** PC1 vs. PC3 (bottom). Branches leading to, as well as the location of terminal taxa in phylomorphospace are color-coated according to clade identity. Clade 1 is outlined in brown, Clade 2 is illustrated in purple, Clade 3 is traced in orange. Species ID number correspond to species as indicated in Table 2. Black hollow dot marks root of the phylogeny.

exhibiting more overall size-corrected cranial shape variation in the first three PC axes than either Clade 1 or Clade 3 (Table 3). The shape features that account for the greatest amount of variation in the morphometric data are interpreted through principal components analysis of each

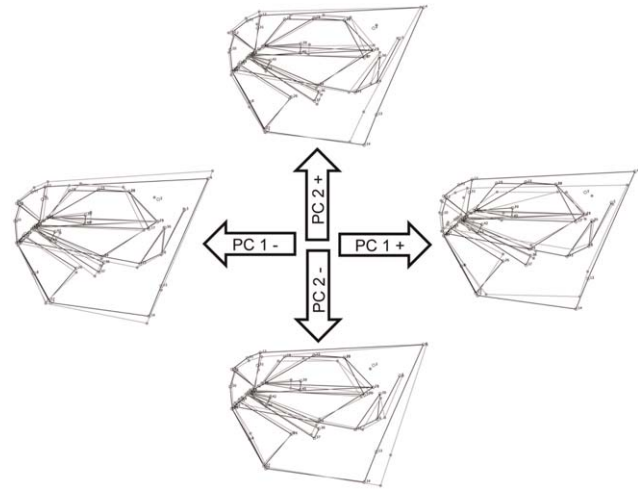


Fig. 5. Major cranial shape changes among triggerfishes calculated using principal components analysis of Procrustes-transformed size-corrected shape data. Black represents consensus triggerfish shape. Grey corresponds to the observed shape variation described by the positive and negative extremes of each of the first two PC axes.

species' average size-corrected Procrustes-superimposed coordinate configuration. The first three PC axes describe 66.64% of the overall variation in the shape data and will hereafter be considered the main descriptors of balistid size-corrected cranial morphospace. Figure 5 illustrates the shape features that scale to the first two PC axes of shape variation using wireframe diagrams. The major axes of shape variation from the evolutionary principal components analysis largely mirror the major sources of interspecific shape variability described by the original PCA shown in Figure 5.

Principal component axis 1 describes 36.584% of the overall cranial shape variation, with triggerfish clades 2 and 3 showing a pattern of diversification throughout a large portion of phylomorphospace PC axis 1. This axis separates fishes with a terminal mouth and a shallow elongate cranial profile that fall out at its positive extreme (all fishes in the genera *Rhinecanthus* and *Sufflamen*) from triggerfishes with a slightly upturned mouth, an overbite, and a steep, rounded cranial profile, which occupy the negative portion on PC1 phylomorphospace (all other triggerfish

TABLE 3. Coefficient of variation scores for the first three axes of size-corrected PC scores pooled within each clade separately  $\pm$  standard error

PC axis	Coefficient of variation for Clade 1	Coefficient of variation for Clade 2	Coefficient of variation for Clade 3
1	0.1055 $\pm$ 0.0094	1.7007 $\pm$ 0.0101	1.3441 $\pm$ 0.0190
2	0.1243 $\pm$ 0.0119	3.6974 $\pm$ 0.0162	3.5070 $\pm$ 0.0098
3	0.4771 $\pm$ 0.0054	2.7821 $\pm$ 0.0125	1.5460 $\pm$ 0.0072

In all three calculations, Clade 2 has a larger coefficient of variation, suggesting that the size-corrected cranial shapes within this clade are more variable, overall, than those in either Clade 1 or Clade 3.

genera). The positive and negative limits of PC1 separates species with the longest Procrustes and Mahalanobis distances between their mean size-corrected shape score (*Rhinecanthus aculeatus* and *Pseudobalistes viridescens*; Procrustes distance = 0.2302,  $P = 0.1032$ ; Mahalanobis distance = 50.657,  $P = 0.0699$ ). On the other hand, those species with the shortest Procrustes and Mahalanobis distance between them, *Sufflamen verres* and *Sufflamen fraenatum*, fall out in similar portions of phylomorphospace along all relevant PC axes (Procrustes distance = 0.0424,  $P = 0.5983$ ; Mahalanobis distance = 12.669,  $P = 0.1019$ ). Interestingly, the cranial shape of *Balistapus undulatus* has converged upon that of fishes in the genera *Rhinecanthus* and *Sufflamen* in the positive portion of PC1 phylomorphospace. The three most convergent species pairs (*Pseudobalistes flavimarginatus* + *Balistes fuscus*, *Canthidermis maculata* + *Melichthys niger*, and *Balistapus undulatus* + *Sufflamen fraenatum*), analyzed for convergence in 2D-morphospace using PC-scores for axes 1–3, had a Wheatsheaf index of 1.12, a level of convergence significantly different from that expected by chance ( $P = 0.04$ ).

Coinciding with gross differences in the overall cranial profile are a number of modifications to the size, shape, and line of action of the adductor mandibulae muscle complex. Most notably, fishes occupying the positive morphospace on PC1 have more dorsoventrally compressed, elongate promalaris, retromalaris, and subrictalis subdivisions, protractor hyoidei superficialis, as well as hyoid musculature relative to the consensus triggerfish shape. All of these muscles insert onto the jaws at a relatively shallow angle. Interestingly, despite the dorsoventral shallowness of *Rhinecanthus*, *Sufflamen*, and *Balistapus*, the substegalis muscle is deeper and shorter in these fishes. The relative location of muscle insertions onto the dentary and maxilla and the size and trajectory of the epistegalis are largely conserved along PC-axis 1.

Principal component 2 describes an additional 20.029% of total shape variation in the size-corrected cranial shape data. Members of triggerfish Clade 2 span from the positive to the negative extremes of phylomorphospace PC2. Members of the genera *Canthidermis* and *Xanthichthys* plot to the negative portion of this axis of morphospace. These fishes exhibit small jaws and teeth, as well as pectoral fins and an opercular complex that are attached farther back along the body axis. Furthermore, the quadrate-articular and premaxilla-palatine jaw joints are closer to the ventral and dorsal borders of the skull, respectively. The overall configuration of the adductor mandibulae muscles varies greatly along PC2. At the positive extreme, the adductor muscles, especially the epirictalis, are “fanned out,” such that the muscle insertions are closer to one another along the jaw bones, whereas the muscle

origination sites span a greater dorsoventral proportion of the ethmoid, frontal, prefrontal and preopercular bones. Interestingly, there are several instances of extreme size-corrected shape divergence along PC-axis 2.

A further 10.031% of overall variation is described by PC-axis 3. Unlike the first two major axes of shape variation, there is more convergence of all balistid clades onto near zero-values on PC3. *Odonus niger* and *Melichthys vidua* occupy the negative extreme, whereas *Pseudobalistes viridescens*, *Sufflamen chrysopterum*, *Canthidermis maculata*, and *Canthidermis sufflamen* fall out along the positive portion of the third PC-axis. The positive morphospace features fishes with origins of both the pars promalaris and pars retromalaris that are positioned farther anteriorly along the ethmoid, steeply sloped ventral cranial elements, and a notably larger upper jaw. The configuration of the pars rictalis and pars substegalis subdivisions varies little along PC3.

### Biomechanical Analyses

Measurements of the jaw lever moment arms varied considerably among the 27 species included in this dataset (Table 1; Figs. 1d–f; 6 and 7). In all species, the morphological mechanical advantage of the upper jaws was higher than that of the lower jaw attachment. Upper jaw mechanical advantage ranged from 0.553 in *Balistes capriscus* to 1.067 in *Xanthichthys auromarginatus*. Lower jaw mechanical advantage spanned from 0.334 in *Sufflamen bursa* to 0.646 in *Odonus niger*.

### DISCUSSION

The evolution of the skull and the complex system of muscles and mechanisms in the feeding apparatus of triggerfishes provides a unique view of skull diversification and the functional role of highly subdivided musculature. The Balistidae have uniquely fused and robust oral jaws powered by a series of architecturally complex, extensively subdivided adductor mandibulae muscles that intricately function together to forcefully close the upper and lower jaws, two bones that are anatomically coupled via the maxillomandibular ligament in balistids. This study presents the first in-depth quantitative morphological analysis of interspecific cranial shape variability in the triggerfish lineage and the biomechanical consequences thereof. Results suggest that size, phylogeny, and the functional demands of different feeding habits have strongly influenced evolutionary trends on triggerfish cranial shape diversification. The central conclusions of this research are: 1) the primary axes of triggerfish cranial shape diversity are tall skulls with relatively short snouts at one extreme and slender long snouted taxa at the other extreme; 2) major triggerfish clades have evolved to occupy

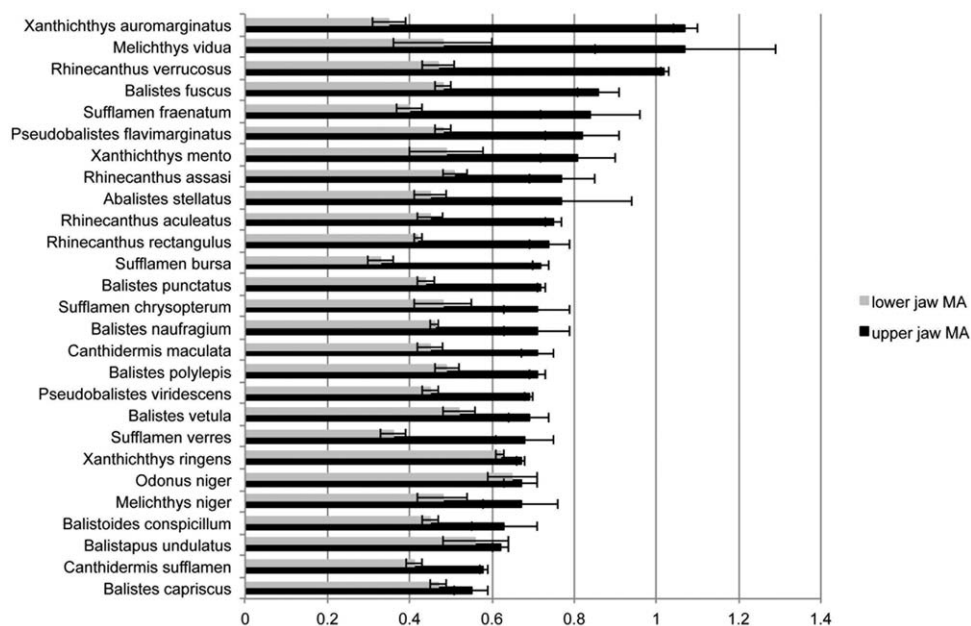


Fig. 6. Each species' mean upper (black) and lower (grey) jaw mechanical advantage. Error bars represent the standard error for each species' values.

overlapping but different sized regions of cranial morphospace, with phylomorphospace position strongly associated with feeding ecology but not necessarily jaw biomechanics; and 3) several instances of convergent evolution and pronounced divergence of the skull morphospace location between closely related species are observed in the triggerfish lineage.

### Evolutionary Trends in Triggerfish Cranial Shape Diversification

The detailed phylomorphospace analyses of extant triggerfishes we present above show that major changes to the overall cranial silhouette and the geometry of functionally relevant morphological skull landmarks have occurred over time in the triggerfish lineage. Interestingly, however, triggerfish skull shape has not diversified to fill all regions of balistid phylomorphospace (Fig. 4). Rather than spreading to fill a broad cloud in morphospace, as is common in skull morphometric analyses from a variety of other taxa, from fishes (Cooper and Westneat, 2009) to lizards (Stayton, 2005) and cats (Sicuro, 2011), triggerfish skull shape evolution has been limited to a T-shaped region of phylomorphospace. The major axis of diversification is one of tall, anteroposteriorly shortened cranial profile in contrast to shallower, more elongate skull morphology. Fishes with deep, stout skulls have adductor muscles that are also short and stout, and attach onto the jaws at steeper angles, whereas fishes with an elongate,

shallow skull exhibit elongate adductor muscles that insert at shallow angles onto the jaws. Phylomorphospace plots suggest that the morphological limits of the major axis of cranial shape variation were established during a burst of morphological evolution that occurred near the root of the triggerfish phylogeny in all major triggerfish clades. More derived portions of the triggerfish lineage have since oscillated within these morphological maximums of skull morphospace. Through this pattern of morphological evolution, we find that the species of Clade 1 have invaded a significantly smaller portion of morphospace and exhibit less shape variation overall than those in Clades 2 or 3 (Fig. 4; Table 3).

Each species' location in phylomorphospace, the shape distance between species, and the results of leave-one-out cross-validation discriminant function analysis provide three complimentary lines of evidence to suggest that shape and genetic differentiation have mostly occurred in parallel through evolution (Fig. 4, Supporting Information). While gradual morphological transformation is certainly the broad pattern of cranial shape evolution in Balistidae, we find instances of both prominent shape diversification among triggerfishes that our previous phylogenetic analyses (McCord and Westneat, 2016) have shown to be closely related, and also significant convergence onto similar regions of morphospace by patristically disparate taxa. In our analyses, cranial shape convergence often appears to be the result of a rapid separation of closely related species in opposite directions in

TABLE 4. Two metrics of evaluating shape variation among the average size-corrected cranial shape of durophagous, generalist and algae/plankton eating triggerfishes

	Algae/plankton	Durophagous	Generalist
Algae/plankton	X	11.3464*	16.6143*
Durophagous	0.1009*	X	14.9775*
Generalist	0.0975*	0.1035*	X

Values below the diagonal Xs are the Procrustes distance between the three feeding guilds; those above are the Mahalanobis distance. \* =  $P$  value  $< 0.05$  from permutation test for Procrustes and Mahalanobis distances among the different feeding guilds.

cranial shape space toward the region in phylomorphospace that is occupied by distantly related triggerfishes with the same dietary habit (Fig. 8). Such is the case in two out of the three significant instances of cranial shape convergence we identified (*Balistapus undulatus* + *Sufflamen fraenatum* and *Pseudobalistes flavimarginatus* + *Balistes fuscus* species pairs). Furthermore, we note that this rapid local divergence resulting in global convergence scales most strongly to the shape features described by PC axis 2, namely the position of the mouth opening and location of jaw joints. Both of these morphometric features have potential biomechanical implications related to the functional demands of capturing and processing different prey items.

While ecomorphological trends are often linked we also find instances of shape convergence, as well as discernable separation of sister species, in morphospace that do not appear to be associated with feeding habits. *Canthidermis maculata* (a generalist) converges significantly onto the same portion of cranial phylomorphospace occupied by *Melichthys niger*, a planktivorous triggerfish. To cross over into the bottom left quadrant of PC1 and PC2 phylomorphospace, it is apparent that the cranial shape of *Canthidermis maculata*, along with that of its sister species *Canthidermis sufflamen*, differ significantly from their closely related clade of generalist fishes in the genera *Abalistes*, *Rhinecanthus*, and *Sufflamen* (Fig. 8). In this example, factors other than recent evolutionary divergence or shared ecology have resulted in the convergence upon similar cranial shape and jaw biomechanics. We predict that differential feeding behavior or divergent adductor muscle activation patterns may be what allows triggerfishes that have similar cranial shape to feed upon different prey items (Wainwright and Friel, 2000).

A second prominent shape diversification pattern occurs among fishes in the exclusively durophagous Clade 1. While *Balistes punctatus*, *Balistes polylepis*, *Balistes capricus*, and *Balistes vetula* all cluster in the same region of phylomorphospace, *Balistes fuscus* and *Balistes naufragium* converge significantly upon their distant relative

*Pseudobalistes flavimarginatus* in a region of phylomorphospace that is significantly divergent from other fishes in Clade 1 according to all multivariate measures of shape variation used in this study (Supporting Information). This example provides an additional layer of evidence that suggests that shared specialist feeding habits are not always sufficient to constrain triggerfishes to a particular region of phylomorphospace. However, it is possible that *Balistes fuscus*, *Balistes naufragium*, and *Pseudobalistes flavimarginatus* are clustering together in phylomorphospace due to some other combination of shared ecological characteristics. In particular, *Balistes naufragium* and *Balistes fuscus* are known to achieve larger body sizes and spend a larger portion of their time in the pelagic zone than the other fishes in Clade 1 (Kuitert and Debelius, 2007). Although *Pseudobalistes flavimarginatus*, *Balistes naufragium*, and *Balistes fuscus* are durophagous, perhaps their foraging behaviors and specific prey preferences are notably different from the other durophagous fishes in this study, thus necessitating a differently configured skull.

### Triggerfish Cranial Shape and Feeding Ecology

The Balistidae have conventionally been identified as durophagous, and there is certainly evidence to suggest that many species are capable of producing the crushing forces necessary for physically breaking down hard shells (Turingan and Wainwright, 1993; Turingan et al., 1995; Friel and Wainwright, 1999). There is also data to suggest that triggerfishes may be accurately assigned to one of three main dietary habits: plankton/algae, durophagy, and generalist (Kuitert and Tonozuka, 2001). If these results are considered within the context of these three ecological groupings, there is clearly some ecological structure to patterns of triggerfish cranial shape diversification. Fishes that eat different things have dissimilar cranial shapes (Fig. 1d–f). We find that the specialists fill a narrower portion of morphospace than do the generalists, which occupy the entirety of PC axis 1 (Fig. 8).

Feeding ecology imposes a strong signal, second only to phylogeny, on patterns of triggerfish morphospace occupation. Noted patterns of shape variation that appear to be influenced by feeding ecology consist of either distantly related fishes that are part of the same feeding guild converging onto the same region of phylomorphospace, or closely related species with different feeding habits rapidly splitting into significantly different portions of phylomorphospace. Geometric morphometric and ecomorphological studies of cichlids (Cooper et al., 2011), wrasses and parrotfishes (Smith et al., 2008; Price et al., 2010), and damselfishes (Cooper and Westneat, 2009) found that

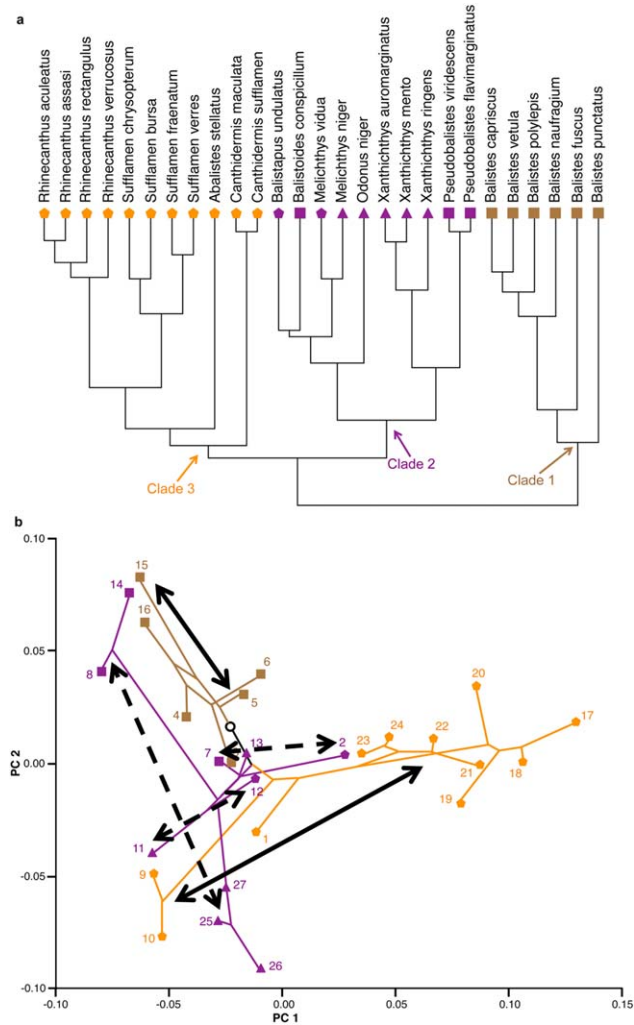


Fig. 7. Diet optimized onto the triggerfish phylogeny **a**) and ecological phylomorphospace plot **b**). Black circle is tree's root. Branches leading to, as well as the location of terminal taxa in ecological phylomorphospace are color-coated according to clade identity. Clade 1 is outlined in brown, Clade 2 is illustrated in purple, Clade 3 is traced in orange. Terminal node symbol identifies feeding guild as illustrated in (a), algae/plankton: triangle; durophagous: square; generalist: pentagon. Species ID number correspond to species as indicated in Table 2. Arrows connected by a dotted line illustrate marked divergence between closely related species that belong to different feeding guilds. Arrows connected by a solid line mark taxa that have diverged in spite of shared feeding habits.

ecological similarity was commonly the underlying cause of convergence upon similar cranial features. We suspect that in the instances of cranial shape convergence and divergence discussed here, the functional demands of feeding habits are the driving factors underlying cranial shape similarity or differences, respectively.

The most extreme and significant ( $P = 0.04$ ) example of independent evolution of similar cranial shape in phylogenetically distant taxa occurs between *Balistapus undulatus* (generalist)

and *Sufflamen fraenatum* (generalist). *Balistapus undulatus* is the only fish phylogenetically within Clade 2 that crosses over into the area of phylomorphospace otherwise occupied exclusively by fishes in the exclusively generalist genera *Rhinecanthus* and *Sufflamen*, both of which are in Clade 3. No fishes from Clade 1 cross over into the positive portion of PC1 phylomorphospace. While *Balistapus undulatus* converges significantly onto shape space occupied by other generalists, all multivariate analyses of shape changes show that it also *diverges* significantly from its durophagous sister species, *Balistooides conspicillum* (Fig. 8; Supporting Information). A second example of striking divergence between closely related organisms that appears to be due to differing feeding ecology is the durophagous *Pseudobalistes viridescens* + *Pseudobalistes flavimarginatus* group falling out at the opposite extreme of PC2

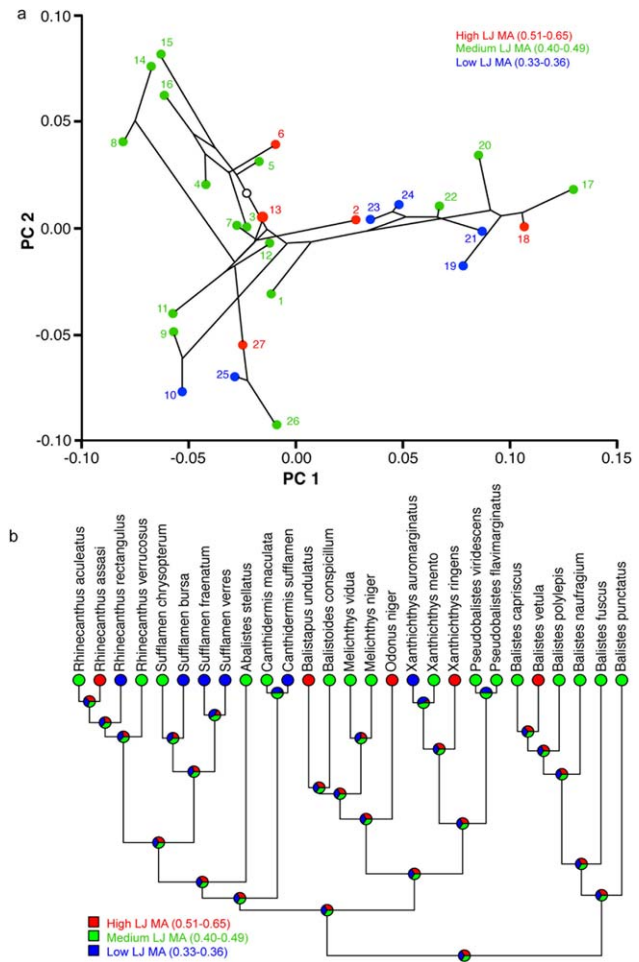


Fig. 8. Functional phylomorphospace plot **a**) and maximum likelihood-based ancestral state reconstruction of lower jaw mechanical advantage onto the triggerfish phylogeny **b**). Black circle is tree's root in functional phylomorphospace plot. Terminal node color identifies high (red), medium (green), or low (blue) lower jaw mechanical advantage. Species ID number correspond to species as indicated in Table 2.

phylomorphospace as their planktivorous sister clade, consisting of fishes in the genus *Xanthichthys*. Members of triggerfish Clade 2 diverge according to feeding guild along PC2 and converge upon the cranial shape space occupied by other fishes that share their respective feeding habits (Fig. 8).

There is also ecological structure to broader patterns of triggerfish phylomorphospace occupation; generalists fall out along the entirety of PC axis 1, whereas both durophagous and algae/plankton eating fishes are limited to the negative region of this axis. As such, durophagous and algae/plankton eating triggerfishes both have short and stout cranial and adductor mandibulae profiles. Principal component 2 splits the algae/plankton eaters, in negative PC2 phylomorphospace, from durophagous fishes that occupy the positive portion of this PC axis. By repeating canonical variate and discriminant function analyses of shape-corrected cranial shape using diet to group fishes, we find that all three dietary groups are shaped significantly different from one another (Table 4). Furthermore, whereas only about 50% of fishes were classified into their correct species through leave-one-out cross-validation, 87.34% of fishes were correctly identified using dietary categories generalist, algae/plankton eater, or durophagous predator. Based upon these results, specialized feeding (as is the case for triggerfishes feeding upon algae/plankton or hard-shelled prey items) may be a limiting factor in the cranial diversification in order to maintain the specific functional demands of planktivory, herbivory, or durophagy.

### Jaw Biomechanics and Trends of the Evolution of Cranial Form and Function in Triggerfishes

The functional capabilities of jaws have been shown to be directly related to the geometric configuration of bones, muscles, and jaw joints in mammals (i.e., Alvarez et al., 2011; Sicuro and Oliveira, 2011; Cornette et al., 2012), reptiles (i.e., Stayton, 2005; Pierce et al., 2008; Marshall et al., 2012), and a large number of fishes (i.e., Wainwright et al., 2004; Westneat et al., 2005; Sidlauskas, 2008; Cooper and Westneat, 2009; Mara et al., 2010; Copus and Gibb, 2013). One of the major findings of this study is that the unique gross anatomy of the triggerfish feeding apparatus has clear biomechanical consequences. Interestingly, however, we find that jaw biomechanical diversity in the balistid lineage is only weakly associated with the phylomorphospace patterns of overall geometric variability in the skull.

The upper jaw rotates in a similar fashion to the mandible (see Fig. 1b,c), enabling us to calculate morphological mechanical advantage of the upper and lower jaws for all species included in this

study. The upper and lower jaws have mechanical advantages that range from 0.483 to 1.072 and 0.334 to 0.646, respectively. Jaw MA values suggest that the upper and lower jaws are capable of transmitting between 33.4 and 107.2% of total potential muscle force through the jaws to the anterior tip of the canine. This is so because a mechanical advantage  $>1.0$ , rare among vertebrates, confers force amplification capacity. These results indicate that the functional capacity of the lower jaw is different from that of the upper jaw; given an equal amount of input force, the upper jaw is capable of transmitting a significantly greater percentage of that force than is the lower jaw. The upper jaw is well suited for stabilizing these high bite forces given the configuration of soft and hard connective tissues associated with the upper jaw joint (see “Results: Triggerfish cranial morphology” for additional details). Several studies have modeled the lower jaw of various fishes as a lever system and calculated the jaw closing mechanical advantage based on the ratio of in-lever to out-lever measurements for the largest lower jaw closing muscle: the retromalaris (also known as the A2). The species average values calculated for the triggerfish lower jaw closing mechanical advantage are among the highest closing MA of all fishes, where previous studies have shown that the closing MA of the lower jaw averages 0.27 (Grubich et al., 2012). Despite variable feeding ecology, the mechanical advantage of triggerfishes is comparable to the anterior MA of durophagous fishes such as parrotfishes (0.45–1.04), chimaeras (0.48–0.68), and horn sharks (0.51) (Wainwright et al., 2004; Huber et al., 2005, 2008). In the largest survey of basic fish jaw biomechanics to date, *Chlorurus sordidus* was found to have the highest jaw closing mechanical advantage with a lever ratio of 0.680 (Westneat, 2004). Eight individuals included in our analyses were found to have a lower jaw MA  $>0.680$ , and the species-averaged lower jaw mechanical advantage for all triggerfishes fell within the range of what the Westneat (2004) study considered “high jaw closing mechanical advantage.”

While both phylogeny and ecology appear to play key roles in shaping patterns of triggerfish phylomorphospace occupation, lever measures of jaw biomechanics are only loosely associated with phylomorphospace. Interestingly, the unique long and skinny cranial shape of fishes in positive PC 1 phylomorphospace does not appear to confer any particular biomechanical consequence; fishes in the genera *Rhinecanthus* and *Sufflamen* have a mixture of high, medium, and low lower jaw mechanical advantages. One pattern we find is that the fishes at the negative extreme of PC axis 1 (those characterized by a short and stout cranium) never achieve a high lower jaw MA. More broadly, high, medium, and low mechanical

advantage values appear throughout the balistid phylogeny, and also in all major quadrants of PC axes 1 and 2 (Fig. 7). High lower jaw mechanical advantage, for example, has evolved independently at least 5 times and at least once in all three major clades in the triggerfish lineage and corresponds to PC scores that span the majority of PC 1 and PC 2. Therefore, both relatively stubby-snouted fishes, such as *Balistes vetula*, and also long and skinny-snouted triggerfishes such as *Rhinecanthus assasi*, achieve high lower jaw mechanical advantage. Furthermore, we found that both the Procrustes and Mahalanobis distances between all three lower jaw MA groups were not significant ( $P > 0.09$  for all discriminant function, canonical variate, and cross-validation tests). On the basis of these findings, we suggest that variable feeding behavior or other measure of jaw biomechanics such as force capacity may be associated with evolutionary patterns of cranial shape transformation in the triggerfish feeding system.

Future work will focus on the development and application of a complex computational model that will calculate additional measures of balistid jaw biomechanics including morphological mechanical advantage, effective mechanical advantage, and force contributions of each of the six triggerfish jaw adductor muscles to total bite force. This model will allow us to quantify the functional role of each muscle subdivision over the course of an entire bite cycle in hopes of further elucidating the evident functional partitioning of force transmission among muscle and directly evaluate the biomechanical consequences of the anatomical coupling of the upper and lower jaws via the maxillomandibular ligament. Because the contractile properties of muscles are known to change in relation to variations in their length (muscle shortening, for example, occurs as the jaws are adducted) dynamic biomechanical models that incorporate the physiological properties of vertebrate skeletal muscle provide powerful computational methods of forming and testing hypotheses relating anatomical structure and biomechanical function (Hill, 1953). Furthermore, the angle at which each muscle inserts relative to the jaw joints changes as the jaws open and close, and will therefore change the effective mechanical advantage, as well as other biomechanical properties (Westneat, 2004). We anticipate each muscle subdivision will have a maximum EMA and effective velocity ratio during different parts of the bite cycle, or at a different point along the tooth row, so as to maintain high bite force throughout an entire bite cycle and wherever prey is being caught or processed within the oral jaws. For clamping down on elusive prey, or producing high bite force to crush hard-shelled organisms, both of these EMA trade-off scenarios offer potential functional benefits.

In conclusion, the synthesis of geometric morphometrics and biomechanical modeling within a phylogenetic context provides novel insight into the patterns of evolution and the ecological role of muscle subdivisions in triggerfishes. Repeated convergence on similar areas of functional morphospace is intriguing ecologically, highlighting the need for additional research on feeding behavior and the ecological role of triggerfishes in complex coral reef ecosystems. Other families within the order Tetraodontiformes exhibit a wide range of anatomical and ecological biodiversity providing an ideal opportunity to explore the consequences of differing degrees of adductor mandibulae subdivision. The morphometric and biomechanical diversification of triggerfishes can now be compared to corresponding patterns of diversity in their sister-family, Monacanthidae, as well as other tetraodontiform fishes to build this evolutionary story.

## ACKNOWLEDGMENTS

The authors thank Kwang-Tsao Shao and Jeffrey Williams for assisting with the use of specimens and hosting C. McCord in Taiwan and Washington D.C., respectively. The authors also thank the Fishes staff at the Field Museum for their assistance and use of specimens, and Rick Winterbottom for insightful conversations about tetraodontiform cranial musculature.

## LITERATURE CITED

- Alvarez A, Perez S, Verzi DH. 2011. Ecological and phylogenetic influence on mandible shape variation of South American caviomorph rodents (Rodentia: Hystricomorpha). *Biol J Linn Soc* 102:828–837.
- Arbuckle K, Bennett CM, Speed MP. 2014. A simple measure of the strength of convergent evolution. *Methods Ecol Evol* 5: 685–693.
- Archie JW. 1985. Methods for coding variable morphological features for numerical taxonomic analysis. *Syst Biol* 34:326–345.
- Barel CDN. 1982. Towards a constructional morphology of cichlid fishes (Teleostei, Perciformes). *Netherlands J Zool* 33: 357–424.
- Biewener AA. 1989. Scaling body support in mammals: Limb posture and muscle mechanics. *Science* 245:45–48.
- Bjarnason A, Soligo C, Elton S. 2015. Phylogeny, ecology, and morphological evolution in the atelid cranium. *Int J Primatol* 36:513–529.
- Bookstein FL. 1997. *Morphometric Tools for Landmark Data: Geometry and Biology*. Cambridge: Cambridge University Press. 455 p.
- Burleigh JG, Alphonse K, Alverson AJ, Bik HM, Blank C, Cirranello AL, Yu M. 2013. Next-generation phenomics for the tree of life. *PLoS Curr* 5:1–9.
- Carpenter KE, Niem VH. 1999. *FAO species identification guide for fishery purposes. The living marine resources of the Western Central Pacific. Volume 3. Batoid fishes, chimaeras and bony fishes part 1 (Elopidae to Linophrynidae)*. FAO Library.
- Collar DC, Near TJ, Wainwright PC. 2005. Comparative analysis of morphological diversity: Does disparity accumulate at the same rate in two lineages of centrarchid fishes? *Evolution* 59:1783–1794.

- Cooper WJ, Westneat MW. 2009. Form and function of damselfish skulls: Rapid and repeated evolution into a limited number of trophic niches. *BMC Evol Biol* 9:24.
- Cooper WJ, Wernle J, Mann K, Albertson RC. 2011. Functional and genetic integration in the skulls of Lake Malawi cichlids. *Evol Biol* 38:316–334.
- Copus JM, Gibb AC. 2013. A forceful upper jaw facilitates picking-based prey capture: Biomechanics of feeding in a butterflyfish, *Chaetodon trichrous*. *Zoology* 116:336–347.
- Cornette R, Herrel A, Cosson JF, Poitevin F, Baylac M. 2012. Rapid morpho functional changes among insular populations of the greater white-toothed shrew. *Biol J Linnean Soc* 107: 322–331.
- D'Amore DC. 2015. Illustrating ontogenetic change in the dentition of the Nile monitor lizard, *Varanus niloticus*: A case study in the application of geometric morphometric methods for the quantification of shape–size heterodonty. *J Anat* 226: 403–419.
- Datovo A, Vari RP. 2013. The jaw adductor muscle complex in teleostean fishes: Evolution, homologies and revised nomenclature (Osteichthyes: Actinopterygii). *PLoS One* 8:e60846.
- Drake AG, Klingenberg CP. 2010. Large-scale diversification of skull shape in domestic dogs: Disparity and modularity. *Am Natur* 175:289–301.
- Footo M. 1997. The evolution of morphological diversity. *Annu Rev Ecol Syst* 28:129–152.
- Friel JP, Wainwright PC. 1997. A model system of structural duplication: Homologies of adductor mandibulae muscles in tetraodontiform fishes. *Syst Biol* 46:441–463.
- Friel JP, Wainwright PC. 1999. Evolution of complexity in motor patterns and jaw musculature of tetraodontiform fishes. *J Exp Biol* 202:867–880.
- Gregory WK. 1933. Fish skulls: A study of the evolution of natural mechanisms. *Trans Am Philos Soc* 23:75–481.
- Grubich JR, Huskey S, Crofts S, Orti G, Porto J. 2012. Mega-Bites: Extreme jaw forces of living and extinct piranhas (Serrasalminae). *Sci Rep* 2:1–9.
- Hill AV. 1953. The mechanics of active muscle. *Proc R Soc Lond Ser B Biol Sci* 141:104–117.
- Huber DR, Eason TG, Hueter RE, Motta PJ. 2005. Analysis of the bite force and mechanical design of the feeding mechanism of the durophagous horn shark *Heterodontus francisci*. *J Exp Biol* 208:3553–3571.
- Huber DR, Dean MN, Summers AP. 2008. Hard prey, soft jaws and the ontogeny of feeding mechanics in the spotted ratfish *Hydrolagus collii*. *J R Soc Interface* 5:941–953.
- Klingenberg CP. 2008. Morphological integration and developmental modularity. *Annu Rev Ecol Evol Syst* 39:115–132.
- Klingenberg CP. 2011. MorphoJ: An integrated software package for geometric morphometrics. *Mol Ecol Resources* 11:353–357.
- Klingenberg CP, Duttke S, Whelan S, Kim M. 2012. Developmental plasticity, morphological variation and evolvability: A multilevel analysis of morphometric integration in the shape of compound leaves. *J Evol Biol* 25:115–129.
- Klingenberg CP, Ekau W. 1996. A combined morphometric and phylogenetic analysis of an ecomorphological trend: Pelagization in Antarctic fishes (Perciformes: Nototheniidae). *Biol J Linnean Soc* 59:143–177.
- Klingenberg CP, Gidaszewski NA. 2010. Testing and quantifying phylogenetic signals and homoplasy in morphometric data. *Syst Biol* 59:245–261.
- Klingenberg CP, Monteiro LR. 2005. Distances and directions in multidimensional shape spaces: Implications for morphometric applications. *Syst Biol* 54:678–688.
- Konstantinidis P, Harris MP. 2011. Same but different: Ontogeny and evolution of the musculus adductor mandibulae in the Tetraodontiformes. *J Exp Zool B Mol Dev Evol* 316:10–20.
- Kuiter RH, Debelius H. 2007. *World Atlas of Marine Fishes*. Frankfurt: Ikan-Unterwasserarchiv.
- Kuiter RH, Tonzuka T. 2001. *Pictorial guide to Indonesian reef fishes. Zoonetics. Part 3. Jawfishes – Sunfishes, Opistognathidae – Molidae. Zoonetics, Australis. p623–893.*
- Lauder GV. 1979. Feeding mechanics in primitive teleosts and in the halecomorph fish *Amia calva*. *J Zool* 187:543–578.
- Lauder GV. 1985. *Aquatic feeding in lower vertebrates. Funct Vertebr Morphol*. Cambridge, MA: Harvard University Press. 210–229.
- Maddison WP. 1991. Squared-change parsimony reconstructions of ancestral states for continuous-valued characters on a phylogenetic tree. *Syst Biol* 40:304–314.
- Mara KR, Motta PJ, Huber DR. 2010. Bite force and performance in the durophagous bonnethead shark, *Sphyrna tiburo*. *J Exp Zool A Ecol Genet Physiol* 313:95–105.
- Marshall CD, Guzman A, Narazaki T, Sato K, Kane EA, Sterba-Boatwright BD. 2012. The ontogenetic scaling of bite force and head size in loggerhead sea turtles (*Caretta caretta*): implications for durophagy in neritic, benthic habitats. *J Exp Biol* 215:4166–4174.
- McCord CL, Westneat MW. 2016. Phylogenetic relationships and the evolution of BMP4 in triggerfishes and filefishes (Balistoidea). *Mol Phylogenet Evol* 94A:397–409.
- Ming B, Xing-Re Y. 2014. A review of three-dimensional (3D) geometric morphometrics and its application in entomology. *Acta Entomol Sin* 57:1105–1111.
- Monteiro LR. 1999. Multivariate regression models and geometric morphometrics: The search for causal factors in the analysis of shape. *Syst Biol* 48:192–199.
- Muschick M, Indermaur A, Salzburger W. 2012. Convergent evolution within an adaptive radiation of cichlid fishes. *Curr Biol* 22:2362–2368.
- Nakae M, Sasaki K. 2004. Homologies of the adductor mandibulae muscles in Tetraodontiformes as indicated by nerve branching patterns. *Ichthyol Res* 51:327–336.
- Olsen AM, Westneat MW. 2015. StereoMorph: An R package for the collection of 3D landmarks and curves using a stereo camera set-up. *Methods Ecol Evol* 6:351–356.
- Openshaw GH, Keogh JS. 2014. Head shape evolution in monitor lizards (*Varanus*): Interactions between extreme size disparity, phylogeny and ecology. *J Evol Biol* 27:363–373.
- Pierce SE, Angielczyk KD, Rayfield EJ. 2008. Patterns of morphospace occupation and mechanical performance in extant crocodylian skulls: A combined geometric morphometric and finite element modeling approach. *J Morphol* 269:840–864.
- Price SA, Wainwright PC, Bellwood DR, Kazancioglu E, Collar DC, Near TJ. 2010. Functional innovations and morphological diversification in parrotfish. *Evolution* 64:3057–3068.
- Revell LJ. 2012. Phytools: An R package for phylogenetic comparative biology (and other things). *Methods Ecol Evol* 3:217–223.
- Rohlf FJ. 2010. *tpsDig v2. 16*. Stony Brook: Ecology and Evolution, SUNY. NJ: Stony Brook.
- Santini F, Sorenson L, Alfaro ME. 2013. A new multi-local timescale reveals the evolutionary basis of diversity patterns in triggerfishes and filefishes (Balistidae, Monacanthidae; Tetraodontiformes). *Mol Phylogenet Evol* 69:165–176.
- Schaefer SA, Lauder GV. 1996. Testing historical hypotheses of morphological change: Biomechanical decoupling in loricae of catfishes. *Evolution* 50:1661–1675.
- Schlick-Steiner BC, Steiner FM, Moder K, Seifert B, Sanetra M, Dyreson E, Christian E. 2006. A multidisciplinary approach reveals cryptic diversity in Western Palearctic Tetramorium ants (Hymenoptera: Formicidae). *Mol Phylogenet Evol* 40:259–273.
- Sicuro FL. 2011. Evolutionary trends on extant cat skull morphology (Carnivora: Felidae): A three-dimensional geometrical approach. *Biol J Linnean Soc* 103:176–190.
- Sicuro FL, Oliveira LFB. 2011. Skull morphology and functionality of extant Felidae (Mammalia: Carnivora): A phylogenetic and evolutionary perspective. *Zool J Linnean Soc* 161: 414–462.
- Sidlauskas B. 2008. Continuous and arrested morphological diversification in sister clades of characiform fishes: A phylogenetic approach. *Evolution* 62:3135–3156.
- Smith LL, Fessler JL, Alfar ME, Strelman JT, Westneat MW. 2008. Phylogenetic relationships and the evolution of

- regulatory gene sequences in the parrotfishes. *Mol Phylogenet Evol* 49:136–152.
- Stayton CT. 2005. Morphological evolution of the lizard skull: A geometric morphometrics survey. *J Morphol* 263: 47–59.
- Tsuboi M, Gonzalez-Voyer A, Kolm N. 2014. Phenotypic integration of brain size and head morphology in Lake Tanganyika Cichlids. *BMC Evol Biol* 14:39.
- Turingan RG. 1994. Ecomorphological relationships among Caribbean tetraodontiform fishes. *J Zool* 233:493–521.
- Turingan RG, Wainwright PC. 1993. Morphological and functional bases of durophagy in the queen triggerfish, *Balistes vetula* (Pisces, Tetraodontiformes). *J Morphol* 215:101–118.
- Turingan RG, Wainwright PC, Hensley DA. 1995. Interpopulation variation in prey use and feeding biomechanics in Caribbean triggerfishes. *Oecologia* 102:296–304.
- Tyler JC. 1980. Osteology, phylogeny, and higher classification of the fishes of the order Plectognathi (Tetraodontiformes) (Vol. 434). US Dept. of Commerce, National Oceanic and Atmospheric Administration, National Marine Fisheries Service.
- Wainwright PC, Friel JP. 2000. Effects of prey type on motor pattern variance in tetraodontiform fishes. *J Exp Zool* 286: 563–571.
- Wainwright PC, Turingan RG. 1993. Coupled versus uncoupled functional systems: Motor plasticity in the queen triggerfish *Balistes vetula*. *J Exp Biol* 180:209–227.
- Wainwright PC, Bellwood DR, Westneat MW, Grubich JR, Hoey AS. 2004. A functional morphospace for the skull of labrid fishes: Patterns of diversity in a complex biomechanical system. *Biol J Linnean Soc* 82:1–25.
- Westneat MW. 1994. Transmission of force and velocity in the feeding mechanisms of labrid fishes (Teleostei, Perciformes). *Zoomorphology* 114:103–118.
- Westneat MW. 2004. Evolution of levers and linkages in the feeding mechanisms of fishes. *Integr Comp Biol* 44:378–389.
- Westneat MW, Alfaro ME, Wainwright PC, Bellwood DR, Grubich JR, Fessler J, Clements KD, Smith L. 2005. Local phylogenetic divergence and global evolutionary convergence of skull biomechanics in reef fishes of the family Labridae. *Proc Roy Soc B* 272:993–1000.
- Winterbottom R. 1974. The Familial Phylogeny of the Tetraodontiformes (Acanthopterygii: Pisces): As Evidenced by Their Comparative Myology. Washington D.C.: Smithsonian Institution Press.
- Zelditch ML, Lundrigan BL, Garland T. 2004. Developmental regulation of skull morphology. I. Ontogenetic dynamics of variance. *Evol Dev* 6:194–206.